



Published in final edited form as:

Nat Chem Biol. ; 8(1): 125–132. doi:10.1038/nchembio.721.

Eukaryotic DNA polymerases require an iron-sulfur cluster for the formation of active complexes

Daili J. A. Netz¹, Carrie M. Stith², Martin Stümpfig¹, Gabriele Köpf¹, Daniel Vogel¹, Heide M. Genau¹, Joseph L. Stodola², Roland Lill^{1,*}, Peter M. J. Burgers^{2,*}, and Antonio J. Pierik^{1,*}

¹Institut für Zytobiologie und Zytopathologie, Philipps-Universität Marburg, Robert-Koch-Strasse 6, D-35033 Marburg, Germany

²Department of Biochemistry and Molecular Biophysics, Washington University School of Medicine, St. Louis, Missouri 63110, USA

Abstract

The eukaryotic replicative DNA polymerases (Pol α , δ , and ϵ), and the major DNA mutagenesis enzyme Pol ζ contain two conserved cysteine-rich metal-binding motifs (CysA and CysB) in the C-terminal domain (CTD) of their catalytic subunits. Here, we demonstrate by *in vivo* and *in vitro* approaches the presence of an essential [4Fe-4S] cluster in the CysB motif of all four yeast B-family DNA polymerases. Loss of the [4Fe-4S] cofactor by cysteine ligand mutagenesis in Pol3 destabilized the CTD and abrogated interaction with the Pol31-Pol32 subunits. Reciprocally, overexpression of accessory subunits increased the amount of CTD-bound Fe-S cluster. This implies an important physiological role of the Fe-S cluster in polymerase complex stabilization. Further, we demonstrate that the Zn-binding CysA motif is required for PCNA-mediated Pol δ processivity. Together, our findings show that the function of eukaryotic replicative DNA polymerases crucially depends on different metalcenters for accessory subunit recruitment and for replisome stability.

Replication of double-stranded nuclear DNA in eukaryotes is performed by the coordinate work of three DNA polymerase complexes, Pol α , δ and ϵ ¹. Pol α together with the primase complex initiates the synthesis of short RNA primers, which are subsequently extended by Pol δ and Pol ϵ for processive synthesis of the lagging and leading strands, respectively^{2,3}. In *Saccharomyces cerevisiae*, Pol α contains four (Pol1, Pol12, Pri1, Pri2), Pol δ three (Pol3, Pol31 and Pol32) and Pol ϵ four (Pol2, Dpb2, Dpb3 and Dpb4) subunits. The catalytic subunits Pol1, Pol2 and Pol3 are phylogenetically related, and belong to the class B DNA polymerases⁴. They are tightly associated with the so-called B subunits Pol12, Dpb2 and

Users may view, print, copy, download and text and data- mine the content in such documents, for the purposes of academic research, subject always to the full Conditions of use: http://www.nature.com/authors/editorial_policies/license.html#terms

*To whom correspondence should be addressed. lill@staff.uni-marburg.de, burgers@biochem.wustl.edu, pierik@staff.uni-marburg.de.

Author contributions All authors performed experiments. D.J.A.N., R.L., P.M.J.B. and A.J.P designed experiments, analyzed data and wrote the manuscript.

Competing financial interests The authors declare no competing interests.

Additional Information Supplementary Information is available online at <http://www.nature.com/naturechemicalbiology/>.

Reprints and permissions information is available online at <http://npg.nature.com/reprintsandpermissions/>.

Pol31, respectively. The B subunits are all essential and share a phosphodiesterase-like and oligosaccharide binding domain^{5,6}. Eukaryotes contain a fourth class B DNA polymerase, Pol ζ , which is the major enzyme responsible for mutagenesis in response to DNA damage^{7,8}. Pol ζ , composed of the catalytic subunit Rev3 and the accessory subunit Rev7, is not essential for growth in yeast, but disruption of *REV3* in mice causes embryonic lethality⁹.

Eight conserved cysteine residues are present in the C-terminal domain (CTD) of all four eukaryotic class B DNA polymerases (Supplementary Fig. 1). This domain is absent in the other classes of DNA polymerases such as bacterial and mitochondrial DNA polymerases. The first set of four cysteine residues (CysA) resembles a Zn ribbon motif (C-X₂-C-X₇₋₃₁-C-X₂-C)¹⁰, whereas the C-terminal set (CysB) has an atypical pattern. This CTD is not present in B-family DNA polymerases of bacteriophages, herpes viruses, proteobacteria and archaea, however, phylogenetic analysis has indicated that a motif similar to CysB is present in the CTD of euryarchaeal D-family polymerases¹¹. The crystal structure of the yeast class B Pol3 has been determined, yet it lacks the entire CTD, since full-length Pol3 isolated from yeast is prone to aggregation¹². Two 3D structures of the CTD of DNA polymerase α have been reported. A Zn²⁺-reconstituted synthetic oligopeptide corresponding to the CysB region of human Pol1 was structurally characterized by NMR spectroscopy¹³. Recently, the crystal structure of the yeast Pol1-CTD in complex with Pol12 was reported¹⁴. This complex was purified from *E. coli* after heterologous expression, and contained a Zn²⁺ ion in both the CysA and CysB motifs. This study provided structural information for earlier biochemical studies which had described interactions between the CTDs and the corresponding B-subunits¹⁵⁻¹⁷.

Intriguingly, the *pol3-13* allele of yeast, in which the second cysteine of CysB (C1074) in Pol3 is mutated to serine, is synthetically lethal with mutations in the essential genes *NBP35*, *DRE2* and *TAH18*¹⁸. These genes encode components of the cytosolic iron-sulfur (Fe-S) protein assembly (CIA) machinery which is required for maturation of most cytosolic and nuclear Fe-S proteins¹⁹⁻²². Nbp35, together with Cfd1, serves as a scaffold complex assembling a transiently bound Fe-S cluster in an early step of the biosynthesis process^{23,24}. Dre2, an Fe-S protein, and the diflavin reductase Tah18 form an electron transfer chain using NADPH for Tah18-dependent reduction of one of the two Fe-S clusters of Dre2²². CIA components acting later in biogenesis encompass the Fe-only hydrogenase-like Nar1 and the β -propeller protein Cia1^{25,26}. Remarkably, the CIA machinery requires a sulfur-containing compound exported by mitochondria after synthesis by the cysteine desulfurase complex Nfs1-Isd11 and other components of the mitochondrial Fe-S cluster (ISC) assembly machinery^{19,27}.

Although it is widely believed that both CysA and CysB of Pol3 bind Zn²⁺ ions, the synthetic lethality between the *pol3-13* allele and mutations in CIA components pointed to the presence of a hitherto unrecognized Fe-S cluster in Pol3. We therefore addressed the question of whether the CTD domain of polymerases may coordinate an Fe-S cluster and what the physiological role of such a cofactor might be. We provide *in vivo* and *in vitro* evidence that a [4Fe-4S] cluster rather than Zn²⁺ is bound to the CysB motif in all yeast B-family DNA polymerases. Assembly of this essential Fe-S cluster was strictly dependent on

the function of mitochondrial Nfs1 and cytosolic Nbp35, explaining the synthetic lethality of the *pol3-13* allele and Fe-S biosynthetic genes¹⁸. The findings also indicate a so far unknown dependence of nuclear DNA synthesis on mitochondrial function. Finally, our study reveals the physiological importance of the two different metal cofactors, the [4Fe-4S] cluster in CysB and Zn²⁺ in CysA, in the stabilization of DNA polymerase interactions with different accessory proteins essential for processive DNA synthesis at the replication fork.

RESULTS

Eukaryotic DNA polymerases bind an Fe-S cluster *in vivo*

To investigate the presumed presence of Fe-S clusters in eukaryotic DNA polymerases, we employed a sensitive *in vivo* radiolabelling assay which measures the incorporation of ⁵⁵Fe into newly synthesized proteins in baker's yeast. The coding information for a C-terminal Myc tag was fused by chromosomal integration to Pol1, Pol2, Pol3, and Rev3, the catalytic subunits of Pol α, ε, δ, and ζ complexes, respectively. No negative effects on growth of the cells were observed by introducing these tags. A significant amount of ⁵⁵Fe was associated with Pol1, Pol2 and Pol3 immunoprecipitated with anti-Myc beads (1.01 ± 0.19 , 1.34 ± 0.17 and 2.6 ± 0.2 pmol/g cells above respective control levels; Fig. 1a and Supplementary Fig. 2). The radiolabelling was not due to adventitiously bound iron to cysteine-rich proteins, since negligible amounts of ⁵⁵Fe bound to transcription factor IIIA (TFIIIA) which contains nine conserved zinc fingers (Fig. 1a). The presence of Fe-S clusters rather than other forms of iron was tested by measuring the dependence of ⁵⁵Fe binding on the mitochondrial and cytosolic Fe-S protein assembly machineries. Depletion of the cysteine desulfurase Nfs1^{19,27} by growth on glucose of the galactose-regulatable strain Gal-*NFS1* almost completely abolished ⁵⁵Fe binding to the polymerases. Proper assembly of the ⁵⁵Fe-S cluster required mitochondria-localized Nfs1, because a cytosolic version of Nfs1 failed to support radiolabelling of Pol3 (Supplementary Fig. 3). Similarly, depletion of the CIA machinery components Nbp35 and Nar1 in regulatable yeast strains (Gal-*NBP35*²⁰ and Gal-*NAR1*²⁵) abrogated Fe-S cluster formation on the polymerases (Fig. 1a and **Supplementary Figs. 2** and 4). Since Pol1 is associated with primase, which contains a [4Fe-4S] cluster in its Pri2 subunit²⁸, the Pri2 contribution to ⁵⁵Fe binding of Pol1 was examined. Although the amount of ⁵⁵Fe co-purified with HA-tagged Pri2 (1.12 ± 0.28 pmol ⁵⁵Fe/g cells) was similar to that measured in Pol1-Myc (1.01 ± 0.19 pmol ⁵⁵Fe/g cells), only 20% of HA-Pri2 co-immunoprecipitated with Pol1-Myc, and vice versa (Supplementary Fig. 5). Thus, a major contribution from Pri2 to Pol1-associated ⁵⁵Fe radioactivity could be excluded. A similar reservation does not hold for Pol δ or Pol ε. None of the small subunits of Pol ε possess conserved cysteine residues as potential ligands for an Fe-S cluster. Structural studies of the small subunits of Pol δ do not indicate the presence of potential metal binding sites⁶. Taken together, our data clearly suggested the presence of a hitherto unrecognized Fe-S cluster in all three replicative DNA polymerase *in vivo*.

The CTD of the catalytic subunit binds the Fe-S cluster

We next tested whether the Fe-S cluster is associated with the CTD, as suggested by the synthetic lethality of the *pol3-13* allele¹⁸ and the strict conservation of the cysteine residues. Since Pol3 is an essential gene and episomal copies of full-length polymerases have

deleterious effects on cell growth²⁹, we expressed only the CTD of Pol3 (amino acids 982-1097) with a N-terminal HA epitope tag from a plasmid. HA-Pol3-CTD bound significant amounts of ⁵⁵Fe (4.1 ± 0.9 pmol/g, Fig. 1b and Supplementary Fig. 6), which dropped to background values in both Nfs1- and Nbp35-depleted cells. This behavior closely resembled that of full-length Pol3 (Fig. 1a). Since no significant ⁵⁵Fe binding to full-length Rev3 could be detected, apparently due to its low abundance (Supplementary Fig. 7), we examined ⁵⁵Fe binding to HA-tagged Rev3-CTD (amino acids 1374-1504). In this case, a significant amount of ⁵⁵Fe (0.9 ± 0.3 pmol/g) was detected, which dropped to background values upon Nfs1 and Nbp35 depletion (Fig. 1b). These results provide evidence that *in vivo* all yeast B-class DNA polymerases bind Fe-S clusters in their CTD. Considering the high amino acid sequence conservation of the CTD of all eukaryotic B-class polymerases¹¹(Supplementary Fig. 1), we anticipate that the presence of an Fe-S cluster in polymerase CTDs extends to all eukaryotes including humans.

Accessory subunits stabilize the Fe-S cluster in CysB

To identify which of the eight conserved Cys residues of the polymerase CTDs are responsible for Fe-S cluster coordination, we used Pol3 as a prototype polymerase, and introduced cysteine to alanine substitutions. In principle, the CysA and CysB motifs may independently bind an Fe-S cluster, as the corresponding segments are structurally well separated (47 Å Zn-Zn distance) by a three-helix bundle in the Zn-bound form of Pol1-CTD¹⁴. All cysteine residues of CysB were required for Fe-S cluster binding *in vivo*, because their substitution by alanine completely abolished ⁵⁵Fe incorporation into Pol3-CTD (Fig. 2a, **right**). In contrast, ⁵⁵Fe binding was significantly above background values for all cysteine to alanine exchanges in CysA suggesting that some Fe-S cluster may still be bound to CysB (Fig. 2a, **left**). The weakened Fe-S cluster binding efficiency of CysA mutant proteins could be caused by a lack of polymerase complex stabilization by Pol31, even though this subunit interacts primarily with the CysB region¹⁷. Indeed, overexpression of Pol31 resulted in a 4- to 8-fold higher ⁵⁵Fe binding to both wild-type and CysA mutant Pol3-CTDs (Fig. 2a and Supplementary Fig. 8) but not to CysB mutant proteins. Nevertheless, the higher levels of Pol31 could not completely compensate for the Fe-S cluster binding deficit caused by cysteine residue exchanges in CysA. We attribute the lower ⁵⁵Fe content of the CysA mutant proteins to an indirect effect of the disruption of the structure of the CysA motif due to the lack of Zn binding. This may affect the efficiency of Fe-S cluster formation in CysB. The decreased protein levels of the CysB-mutated CTD domain found in immunostains of cell extracts, even upon Pol31 overexpression (Supplementary Fig. 8 a,c), can be explained by the absence of the Fe-S cluster in CysB. This rendered the protein sensitive to degradation, as frequently seen for Fe-S proteins. Together, these findings imply that only CysB is responsible for Fe-S cluster binding, whereas CysA may bind zinc¹⁴. We infer that Pol3-Pol31 complex formation is intrinsically linked to the presence of an intact Fe-S cluster, explaining its physiological importance for Pol δ function.

Next, we tested whether the functional connection between the presence of an Fe-S cluster on the DNA polymerase and its interaction with the respective accessory subunits also holds for the other B-class family members. Overexpression of Pol12, Dpb2 and Rev7 with the

CTDs of Pol1, Pol2 and Rev3, respectively, significantly increased the amounts of ^{55}Fe co-isolated in the absence of the over-produced accessory subunits (Fig. 2b). Thus, the increase in the efficiency of Fe-S cluster binding to the polymerase CTDs by the respective accessory subunits appears to extend to all members of the B class family suggesting a stabilization of Fe-S cluster binding by these subunits and *vice versa*.

The [4Fe-4S] cluster is required for complex formation

To characterize the type and stoichiometry of Fe-S cluster binding to DNA polymerases, we performed biochemical and spectroscopic studies. Expression of the yeast Pol1-, Pol2-, Pol3- and Rev3-CTD in *E. coli* resulted in the formation of dark inclusion bodies, which upon treatment with chaotropic agents gave brownish solutions (Fig. 3a). Soluble brown Pol2-, Pol3-, and Rev3-CTDs could be obtained in the absence of chaotropic agents after modifications of the protocol (Supplementary Fig. 9). Pol1-CTD and Pol2-CTD were aggregation-prone. A low yield of Pol1-CTD holoform was obtained (~0.1 Fe and S per monomer, Supplementary Fig. 10). This apparent lability of Fe-S cluster binding to purified Pol1-CTD may have precluded its earlier discovery in structural studies¹⁴. The other CTDs contained 2.0-2.6 mol non-heme iron and acid-labile sulfide per CTD, and their UV-Vis spectra displayed a broad absorption maximum centered at 400 nm indicative of [4Fe-4S] clusters (Fig. 3b). These soluble CTDs did not show electron paramagnetic resonance (EPR) signals, even after oxidation with ferricyanide, excluding the presence of [3Fe-4S] clusters³⁰. However, upon reduction with dithionite, EPR signals ($g_{\parallel} = 2.04$ and $g_{\perp} = 1.93$) characteristic for [4Fe-4S]¹⁺ clusters were detected (Fig. 3c). Together, these results provide evidence for a single [4Fe-4S]²⁺ cluster bound to the purified CTDs.

Since no Fe-S cluster has been detected in any isolated DNA polymerase complex, we investigated the native Pol δ complex for such a metal centre after induced expression and purification from *S. cerevisiae* (Supplementary Fig. 11 a,b). Isolated Pol δ was olive-yellow and contained Pol3, Pol31 and Pol32 in stoichiometric ratios (Fig. 4a, Supplementary Fig. 11c). UV/Vis spectroscopy of Pol δ showed a broad absorption in the 400 nm region, and chemical analysis detected approximately 4 mol non-heme iron and acid-labile sulfide ions per mol Pol δ (Fig. 4b, inset). Thus, the Fe-S content, the UV-Vis spectrum and the extinction coefficient of $13 \text{ mM}^{-1}\text{cm}^{-1}$ at 400 nm indicated the presence of a single [4Fe-4S]²⁺ or a single [3Fe-4S]¹⁺ cluster in purified Pol δ complex (Fig. 4b). EPR spectroscopy showed a weak signal centered at $g = 2.02$ characteristic for [3Fe-4S]¹⁺ clusters. Spin quantification of the EPR signal, however, accounted for only $5 \pm 1 \%$ of the total Fe-S cluster content (Fig. 4c). This signal increased twofold upon oxidation with ferricyanide, corresponding to just $10 \pm 2 \%$ of the Fe-S cluster content. After dithionite treatment of the wild-type Pol δ complex, the [3Fe-4S]¹⁺ cluster EPR signal at $g = 2.02$ disappeared due to reduction to the EPR-silent [3Fe-4S]⁰ state. However, native Pol δ treated with dithionite did not exhibit a [4Fe-4S]¹⁺ EPR signal. (Fig. 4c, top trace). These findings are in contrast to the results for the soluble CTDs, in which the [4Fe-4S]²⁺ cluster may be reduced to the [4Fe-4S]¹⁺ form. The absence of an EPR signal in dithionite-treated polymerase δ could be explained by a lower redox potential of the [4Fe-4S]²⁺ cluster in the intact complex in comparison to Pol3-CTD. Dithionite can only reduce the cluster if the midpoint potential is above -500 mV , which is apparently the case for the CTDs.

Alternatively, the $[4\text{Fe-4S}]^{1+}$ cluster may have a high spin state with an EPR spectrum too broad to be detectable. A third explanation would be conversion of the $[4\text{Fe-4S}]^{1+}$ cluster to the EPR silent $[3\text{Fe-4S}]^0$ form. Breakdown of the cluster upon dithionite treatment is unlikely, since processivity remained unaltered. Many other $[4\text{Fe-4S}]^{2+}$ cluster-containing proteins have EPR and redox properties similar to native Pol δ . For example, aconitase has a labile $[4\text{Fe-4S}]^{2+}$ cluster that is converted to the $[3\text{Fe-4S}]^{1+}$ form during isolation³¹, and the $[4\text{Fe-4S}]^{2+}$ cluster is difficult to reduce with dithionite. Regardless of the behavior upon dithionite treatment, our analysis provides evidence that Pol δ isolated from yeast contains a $[4\text{Fe-4S}]^{2+}$ cluster, which upon purification partially (5-10 %) breaks down to a $[3\text{Fe-4S}]^{1+0}$ cluster.

To verify the specificity and physiological relevance of Fe-S cluster binding to polymerases, we studied the effect of mutations in CysA or CysB on both Fe-S cluster binding and functionality of isolated Pol δ . The lethal double mutation C1059S/C1074S in CysB of Pol3 disrupted its binding to both Pol31 and Pol32 upon isolation of Pol3 from cell extracts and in yeast two hybrid experiments (Fig. 4a, Supplementary Fig. 12). The mutation further abrogated Fe-S cluster binding as seen from chemical analysis and the loss of UV-Vis and EPR signals (Fig. 4b-c). In marked contrast, lethal double mutation of CysA (C1012S/C1027S) did not alter the subunit composition of the purified Pol δ complex, and did not affect the Pol3 interactions in the two hybrid analysis. Likewise, the Fe-S content, the UV-Vis and EPR spectra were unchanged in comparison to the wild-type situation. These data further support the view that CysB binds a $[4\text{Fe-4S}]$ cluster, while no evidence was obtained for Fe-S cluster binding to CysA. Hence, based on the consensus Zn ribbon motif of CysA (C-X₂-C-X₇₋₃₁-C-X₂-C)¹⁰ and the crystallographic data, CysA may bind zinc¹⁴. Neither set of mutations in the CTD of Pol3 affected its basal DNA polymerase activity (Supplementary Fig. 13), in agreement with Pol3 truncation mapping studies and structural comparisons with other B-family DNA polymerases that localize the catalytic domain N-terminal of the CTD¹².

CysA is an important determinant for PCNA binding

What may be the physiological function of the Zn-binding CysA motif? Processive DNA replication can be tested *in vitro* and depends on multiple protein and protein-DNA interactions including those with the processivity factor, PCNA^{32,33}. The latter protein is a circular homotrimeric clamp that coordinates DNA replication, recombination, and repair processes, and endows both stability and processivity of the replicating machinery. To address the role of the CysA motif in processive, lagging-strand DNA replication, we used isolated Pol δ preparations (Pol3, Pol31, and Pol32; Supplementary Fig. 11) for *in vitro* DNA synthesis in the presence of PCNA (Supplementary Fig. 14). Mutation of two cysteine residues of CysA (C1012S/C1027S) severely decreased PCNA-dependent replication processivity documenting the utmost importance of this metal center for polymerase function (Fig. 5a). An interaction between Pol δ and PCNA has previously been mapped to a C-terminal segment of the accessory subunit Pol32, and termed PIP (PCNA interaction protein) motif³³. However, the Pol32- PIP mutant form of Pol δ was almost fully proficient for processive DNA replication documenting its minor functional importance. The relative effects observed for the Pol3-CysA and Pol32- PIP mutants shows a much higher

importance of the CysA site compared to PIP for stability of the PCNA-polymerase complex on DNA. Hence, the CysA structural motif may represent the key binding site for PCNA on Pol δ , while the PIP motif may have an ancillary function. Consistent with this view, PCNA-dependent replication activity of Pol δ was almost completely abolished when both CysA and PIP binding sites were mutated (Fig. 5a). As controls for these experiments, the catalytic subunit Pol3 alone, the CysB mutant protein, or a sample lacking PCNA showed no discernible processive DNA replication. To further substantiate the relative importance of the two PCNA binding sites of Pol δ , we varied the PCNA concentration in the *in vitro* replication assay containing either wild-type or CysA mutant Pol3 together with wild-type or PIP Pol32. Increasing PCNA concentrations relieved the replication defect of the CysA mutant suggesting that under these conditions interactions between PCNA and PIP partially rescue the replication defect (Fig. 5b). Indeed, when PIP was also absent, hardly any processive replication was observed. Taken together, these findings suggest a crucial role of CysA for PCNA-Pol δ complex formation and/or stability during on-DNA processive DNA replication (Fig. 5c). In contrast, the PIP binding site may be more relevant for off-DNA complex formation, such as recruitment of the enzyme to replication foci in the nucleus, as has been observed with other PIP box-containing proteins^{33,34}.

DISCUSSION

Our study identifies a previously unrecognized essential Fe-S cluster in the CTD of all yeast B-class DNA polymerases, in addition to a Zn²⁺ ion bound on the other side of CTD¹⁴. Hence, this class of enzymes contains two different metal centers which were shown to perform distinct physiological roles. The presence of the Fe-S cluster was demonstrated by several *in vivo* and *in vitro* methods such as ⁵⁵Fe radiolabelling and purification of the DNA polymerase complex after induced expression from yeast, the native organism. Mutational and spectroscopic studies allowed us to define it as a [4Fe-4S] cluster that is coordinated by CysB, the second cysteine-rich motif in the CTD. The presence of an Fe-S cluster rather than Zn²⁺, as originally suggested by a crystal structure of the CTD of Pol1, changes our understanding of DNA polymerase function and raises several questions regarding the precise physiological role of this Fe-S cluster. Our data clearly demonstrate that Pol3 becomes unstable in absence of the Fe-S cluster (e.g., upon Nfs1 depletion, see Western blots of Supplementary Fig. 2) and that the replication function is severely compromised due to loss of accessory subunits essential for function at the replication fork (Fig. 4). This functional impairment caused by decreased complex stability may extend to the other DNA polymerases, because the interaction between the various CTDs and their respective accessory proteins was a key determinant for stability of the bound Fe-S cluster. It is likely that euryarchaeal D-family polymerases also bind an Fe-S cluster in the CysB motif. Interestingly, these polymerases contain a B subunit with phosphodiesterase-like and oligosaccharide binding domains⁶, and are thus predicted to share the principle of Fe-S cluster binding for accessory subunit recruitment with the eukaryotic polymerases. In the case of the translesion polymerase Pol ζ , the accessory protein Rev7 has a fold completely different from the B subunits of the other polymerases, and therefore a firm conclusion by analogy with Pol δ cannot be made and requires direct experimentation. However, the data do suggest that the Rev3-CTD may also be involved in Rev3-Rev7 interactions, in addition

to interaction of the N-terminal region of the polymerase domain of Rev3 with Rev7³⁵. Together, our findings assign an essential role to the Fe-S cluster in stabilizing the CTD to enable complex formation and/or maintenance of the catalytic polymerase subunit with its respective accessory proteins. Since an Fe-S cluster is intrinsically sensitive to oxidative stress, oxidative damage of the cluster may lead to gradual dissociation of the accessory subunits and a decreased processivity at the replication fork. An attenuated rate of DNA replication during oxidative stress conditions may serve as a regulatory mechanism for polymerase activity.

In retrospect, the lability and complexity of Fe-S clusters may explain the previous difficulties in obtaining purified polymerase complex suitable for functional studies and crystallography. Purification of the catalytic subunit on its own invariably resulted in low yields and aggregation (see Methods), possibly explaining why Pol3 could only be crystallized after truncation of the C-terminus¹². The Pol1-CTD in complex with Pol12 was crystallized with a Zn²⁺ ion in CysB after heterologous expression and purification from *E. coli*¹⁴. Our own purification experiments after expression in *E. coli* showed an extreme lability of the Fe-S cluster of Pol1-CTD necessitating anaerobic purification conditions to co-isolate the Fe-S cluster with the protein. In general, misincorporation of non-native metal centers into metallo-proteins is not unusual, and has been encountered especially upon overproduction or heterologous expression of metallo-proteins. For instance, replacement of Fe or an Fe-S cluster by Zn in *E. coli* has been reported for *Clostridium pasteurianum* rubredoxin³⁶ or for the Fe-S cluster-containing scaffold protein IscU from *Haemophilus influenzae*³⁷, respectively. Likewise, the CIA protein Nar1, containing two Fe-S clusters, does not contain its native metal centers after expression in *E. coli*³⁸. Zinc can be erroneously incorporated into the copper-binding protein azurin³⁹. Ribonucleotide reductases of various bacteria, upon overexpression in *E. coli*, contain a dinuclear Fe center, yet in its native state the enzyme possesses a di-manganese center^{40,41}. Hence, these data imply that a number of proteins isolated as Zn-binding proteins, may exist as Fe-S proteins inside the cell, emphasizing the importance of assessing the metal occupancy of a protein in its native organism.

Our data provide evidence for a previously unknown, crucial function for the CysA Zn-binding segment in mediating DNA-dependent interactions between PCNA and the catalytic subunit of Pol δ (Fig. 5c). This protein interaction appears to operate in addition to an earlier defined binding determinant, the C-terminal PIP motif of the accessory subunit Pol32. Since the CysA mutation was more detrimental for *in vitro* processive DNA replication than the deletion of the PIP segment, CysA may be the major determinant for PCNA interaction with Pol δ on DNA. Notably, the function of the CysA motif may be more divergent than that of CysB, which appears to be conserved among all replicative DNA polymerases as a structural motif for the interaction with the respective essential accessory subunits. In Pol δ , Pol ϵ and Pol ζ the CysA motif may serve a similar function, i.e. that of mediating DNA-dependent interactions with PCNA, as all these polymerases require PCNA for processive synthesis^{42,43}. However, functional interactions between PCNA and Pol α have not been demonstrated^{32,44}, and therefore the functional role of the CysA motif in this enzyme awaits further investigation.

Our findings indicate that insertion of the Fe-S cluster into nuclear DNA polymerases not only depends on the function of the cytosolic but also of the mitochondrial Fe-S protein biogenesis machineries (Fig. 6). The cysteine desulfurase Nfs1 located only in the cytosol-nucleus could not assist in the assembly of the Fe-S cluster into Pol3 (Supplementary Fig. 3). Thus, Nfs1, and presumably other members of the mitochondrial ISC assembly machinery¹⁹, need to operate inside mitochondria to support Fe-S cluster insertion into polymerases. This finding surprisingly shows that mitochondria are essential for nuclear DNA replication, presumably acting as a sulfur donor for the DNA polymerase Fe-S cluster discovered here. This crucial task of mitochondria provides an explanation for their indispensable function for cell viability in virtually all eukaryotes and may be more basic than even respiration which is dispensable in some organisms¹⁹. Interestingly, other steps of eukaryotic DNA and RNA metabolism involve Fe-S proteins including factors required for ribosome function in protein translation (Rli1), or for DNA repair, transcription, and chromosome segregation (Rad3/XPD, FancJ, Chl1)¹⁹. On the one hand, this may explain the involvement of mitochondrial function in several DNA metabolism-related, neurodegenerative and cancer-linked phenotypes including nuclear genome instability⁴⁵. At least a subset of these disorders could originate from impaired Fe-S cluster assembly on these proteins and on the B-family DNA polymerases. On the other hand, the indispensable role of mitochondria in nuclear DNA and RNA metabolism suggests that eukaryotes, at some point in evolution, made themselves dependent on these endosymbiotic organelles to express their genome.

METHODS

Yeast strains and plasmids

Saccharomyces cerevisiae W303-1A (*MATa*, *ura3-1*, *ade2-1*, *trp1-1*, *his3-11,15* and *leu2-3,112*) was used as wild type and as background strain for cells with genes under the control of galactose-regulatable promoters and/or encoding N- or C-terminally epitope-tagged proteins. For details of strains and plasmid constructs see Supplementary Methods and Supplementary Tables 1 and 2.

Expression in *E. coli* and purification of CTDs

The pASK-IBA43plus plasmids encoding the C-terminally Strep-tagged CTD domains of Pol1, Pol2, Pol3 or Rev3 were transformed into BL21 *E. coli* cells. Induction with anhydrotetracycline hydrochloride (AHT, 4.3 μ M) was at OD_{600nm} of 0.5-0.7, at 30 °C for 16 h. Under these conditions Pol1, Pol2 and Rev3 were totally insoluble. Inclusion bodies were solubilized in purification buffer (100 mM Tris-Cl pH 8.0, 150 mM NaCl) containing 8 M urea. For Pol2, 6 M guanidinium hydrochloride was used instead of urea. To yield soluble CTDs an overnight culture of *E. coli* HMS174 (DE3) pLysS transformed with pASK-IBA43plus encoding the C-terminally Strep-tagged CTD domains of Pol1, Pol2, Pol3 or Rev3 was diluted 100-fold into Terrific broth containing 3% (v/v) ethanol and allowed to grow to an OD_{600nm} of 0.5 at 37°C. The cultures were cooled down to 20°C (~ 30 min) and benzyl alcohol (1 ml / 1 culture), betaine hydrochloride (1 mM), FeCl₃ (50 μ M) and L-cysteine (100 μ M) were added, followed by AHT. After ~16 h of expression at 20°C the cells were harvested and resuspended in anaerobic purification buffer. All subsequent steps

were conducted in an anaerobic chamber (Coy) maintaining samples at 4 °C. The cell suspension was treated with 0.5 mg lysozyme per g cells for 30 min and disrupted by sonication (three 30 s bursts, with 1 min cooling periods). After centrifugation at 100,000×g for 45 min, the supernatant was mixed with one-tenth of its volume of high capacity Strep-Tactin agarose (IBA) and homogenized for 1 h. The slurry was poured into a column and washed with 10 bed volumes of cold purification buffer, followed by elution with the same buffer containing 2 mM desthiobiotin. The proteins were analyzed by UV-Vis spectroscopy and frozen for EPR spectroscopy immediately after purification. For chemical analysis and SDS-PAGE samples were shock-frozen and stored at –80 °C.

Purification of yeast polymerase δ from yeast cells

Pol δ was purified from a yeast overproduction system⁴⁶. *POL3* containing a cleavable N-terminal GST-purification tag, *POL31*, and *POL32* were overexpressed from the galactose-inducible *GAL1-10* promoter in protease-deficient strain BJ2168 (*MATa*, *ura3-52*, *trp1-289*, *leu2-3,112*, *prb1-1122*, *prc1-407*, *pep4-3*). After affinity purification on glutathione beads and removal of the GST tag by rhinoviral 3C protease, the preparation was further purified on a MonoS column. SDS-PAGE in Fig. 4a and Supplementary Fig. 11c is of the MonoS eluates. Single and double Cys to Ser mutants were made by the Quikchange (Stratagene) protocol. Mutants were subjected to the same purification protocol. Since GST-tagged Pol3 was used for affinity purification, the presence of Pol31 and Pol32 in the Pol3-CysA mutant preparation, and their absence from the Pol3-CysB mutant preparation, indicates retention and defect in Pol3-Pol31 interactions in the mutants, respectively. After concentration to >2 mg/ml using Centricon filters, preparations of the wild-type and the CysA mutant, but not of the CysB mutant, showed an olive-yellow color. The Pol3 catalytic subunit on its own was prepared as described above, but after overexpression employing only the pBL335 plasmid in BJ2168. The yield was invariably low and the protein was aggregation prone. Contaminating three-subunit enzyme was removed by two consecutive MonoS column steps (the single Pol3 subunit elutes prior to Pol δ). Pol δ preparations with Pol32- PIP and containing either the wild-type or CysA form of Pol3, were overproduced in strain PY117 (*MATa*, *ura3-52*, *trp1-289*, *leu2-3,112*, *his3-11,15*, *prb1-1122*, *pep4-3*, *pol32- ::HIS3*), a *pol32* derivative of BJ2168³³. Complex purification was performed in the same way as for wild-type.

Single strand DNA replication assays

PCNA, RFC, and RPA were purified as described⁴⁷⁻⁴⁹. Assays (60 μ l) contained 20 mM Tris-HCl 7.8, 1 mM DTT, 100 μ g/ml bovine serum albumin, 8 mM magnesium acetate, 0.5 mM ATP, 100 μ M each of dCTP, dGTP, and dTTP, 10 μ M of [α -³²P]-dATP, 100 mM NaCl, 2 nM of singly primed (36 bp, complementary to nt 6330–6295) single-stranded M13mp18 DNA, 500 nM of RPA, and 5 nM of PCNA (or indicated PCNA concentration for Fig. 5). PCNA was loaded onto the primed DNA by incubation with 5 nM RFC at 30 °C for 1 min, and replication started by addition of (mutant) Pol δ or Pol3. Aliquots (18 μ l) were taken at various time points and replication was stopped by the addition of 2 μ l 100 mM EDTA and 3% SDS. After incubating at 50 °C for 10 min, 45 μ l of precipitation solution [2.5 M ammonium acetate, 20 μ g/mL sonicated salmon sperm DNA, 1 mM EDTA and 0.05 mg/ml linear acrylamide (Ambion Technologies)] was added, followed by ethanol

precipitation. The dissolved pellet was analyzed by electrophoresis on a 1% alkaline agarose gel. Gels were dried and documented by phosphorimager analysis.

EPR and UV-Vis spectroscopy

EPR spectra were recorded with a Bruker EMX-6/1 X-band spectrometer containing an ER-041 XG microwave bridge, ER-041-1161 frequency counter, EMX-1101 power supply, ER-070 magnet, EMX-032T Hall field probe, ER-4102 Universal TE102 rectangular cavity, and Oxford Instruments helium flow cryostat ESR-900. Data acquisition and manipulation was done with the Bruker WINEPR software. For spin quantification 1 mM CuSO₄ in 2 M NaClO₄ and 10 mM HCl was used. UV-Vis spectra were recorded on a Jasco V-550 spectrophotometer. For EPR and UV-Vis spectroscopy the proteins were in anaerobic purification buffer, treated with sodium dithionite (2 mM) or potassium ferricyanide (2 mM) where applicable. Samples were transferred inside the anaerobic chamber to stoppered anaerobic quartz cuvettes (Hellma) or Ilmasil-PN high purity quartz EPR tubes. EPR samples were capped with rubber seals and shock-frozen outside the anaerobic chamber in liquid nitrogen.

Additional methods

⁵⁵Fe incorporation, cloning, yeast two-hybrid analysis, cysteine mutagenesis, chemical analysis of iron and acid-labile sulfide are described in the Supplementary Methods.

Supplementary Material

Refer to Web version on PubMed Central for supplementary material.

Acknowledgements

We thank Bonita Yoder for yeast two-hybrid analysis and Max Reuter for help with cloning. Supported by grant GM032431 from the National Institutes of Health (P.M.J.B) and the Deutsche Forschungsgemeinschaft (SFB 593, Gottfried-Wilhelm Leibniz program, and GRK 1216), Rhön Klinikum, von Behring-Röntgen Stiftung, LOEWE program of state Hessen, Max-Planck Gesellschaft, and Fonds der chemischen Industrie.

References

1. Johansson E, Macneill SA. The eukaryotic replicative DNA polymerases take shape. *Trends Biochem. Sci.* 2010; 35:339–347. [PubMed: 20163964]
2. Nick McElhinny SA, Gordenin DA, Stith CM, Burgers PM, Kunkel TA. Division of labor at the eukaryotic replication fork. *Mol. Cell.* 2008; 30:137–144. [PubMed: 18439893]
3. Pursell ZF, Isoz I, Lundström EB, Johansson E, Kunkel TA. Yeast DNA polymerase ϵ participates in leading-strand DNA replication. *Science.* 2007; 317:127–130. [PubMed: 17615360]
4. Burgers PM, et al. Eukaryotic DNA polymerases: proposal for a revised nomenclature. *J. Biol. Chem.* 2001; 276:43487–43490. [PubMed: 11579108]
5. Mäkineniemi M, et al. A novel family of DNA-polymerase-associated B subunits. *Trends Biochem. Sci.* 1999; 24:14–16. [PubMed: 10087916]
6. Baranovskiy AG, et al. X-ray structure of the complex of regulatory subunits of human DNA polymerase δ . *Cell Cycle.* 2008; 7:3026–3036. [PubMed: 18818516]
7. Nelson JR, Lawrence CW, Hinkle DC. Thymine-thymine dimer bypass by yeast DNA polymerase ζ . *Science.* 1996; 272:1646–1649. [PubMed: 8658138]

8. Prakash S, Johnson RE, Prakash L. Eukaryotic translesion synthesis DNA polymerases: specificity of structure and function. *Annu. Rev. Biochem.* 2005; 74:317–353. [PubMed: 15952890]
9. Bemark M, Khamlichi AA, Davies SL, Neuberger MS. Disruption of mouse polymerase ζ (Rev3) leads to embryonic lethality and impairs blastocyst development *in vitro*. *Curr. Biol.* 2000; 10:1213–1216. [PubMed: 11050391]
10. Krishna SS, Majumdar I, Grishin NV. Structural classification of zinc fingers: survey and summary. *Nucleic Acids Res.* 2003; 31:532–550. [PubMed: 12527760]
11. Tahirov TH, Makarova KS, Rogozin IB, Pavlov YI, Koonin EV. Evolution of DNA polymerases: an inactivated polymerase-exonuclease module in Pol ϵ and a chimeric origin of eukaryotic polymerases from two classes of archaeal ancestors. *Biol. Direct.* 2009; 4:11. [PubMed: 19296856]
12. Swan MK, Johnson RE, Prakash L, Prakash S, Aggarwal AK. Structural basis of high-fidelity DNA synthesis by yeast DNA polymerase δ . *Nat. Struct. Mol. Biol.* 2009; 16:979–986. [PubMed: 19718023]
13. Evanics F, Maurmann L, Yang WW, Bose RN. Nuclear magnetic resonance structures of the zinc finger domain of human DNA polymerase- α . *Biochim. Biophys. Acta.* 2003; 1651:163–171. [PubMed: 14499601]
14. Klinge S, Núñez-Ramírez R, Llorca O, Pellegrini L. 3D architecture of DNA Pol α reveals the functional core of multi-subunit replicative polymerases. *EMBO J.* 2009; 28:1978–1987. [PubMed: 19494830]
15. Mizuno T, Yamagishi K, Miyazawa H, Hanaoka F. Molecular architecture of the mouse DNA polymerase α -primase complex. *Mol. Cell. Biol.* 1999; 19:7886–7896. [PubMed: 10523676]
16. Dua R, Levy DL, Campbell JL. Analysis of the essential functions of the C-terminal protein/protein interaction domain of *Saccharomyces cerevisiae* pol ϵ and its unexpected ability to support growth in the absence of the DNA polymerase domain. *J. Biol. Chem.* 1999; 274:22283–22288. [PubMed: 10428796]
17. Garcia, J. Sanchez; Ciuflo, LF.; Yang, X.; Kearsey, SE.; MacNeill, SA. The C-terminal zinc finger of the catalytic subunit of DNA polymerase δ is responsible for direct interaction with the B-subunit. *Nucleic Acids Res.* 2004; 32:3005–3016. [PubMed: 15173383]
18. Chanet R, Heude M. Characterization of mutations that are synthetic lethal with *pol3-13*, a mutated allele of DNA polymerase delta in *Saccharomyces cerevisiae*. *Curr. Genet.* 2003; 43:337–350. [PubMed: 12759774]
19. Lill R. Function and biogenesis iron-sulphur proteins. *Nature.* 2009; 460:831–838. [PubMed: 19675643]
20. Hausmann A, et al. The eukaryotic P-loop NTPase Nbp35: An essential component of the cytosolic and nuclear iron-sulfur protein assembly machinery. *Proc. Natl. Acad. Sci. U.S.A.* 2005; 102:3266–3271. [PubMed: 15728363]
21. Zhang Y, et al. Dre2, a conserved eukaryotic Fe/S cluster protein, functions in cytosolic Fe/S protein biogenesis. *Mol. Cell. Biol.* 2008; 28:5569–5582. [PubMed: 18625724]
22. Netz DJA, et al. Tah18 transfers electrons to Dre2 in cytosolic iron-sulfur protein biogenesis. *Nat. Chem. Biol.* 2010; 6:758–765. [PubMed: 20802492]
23. Roy A, Solodovnikova N, Nicholson T, Antholine W, Walden WE. A novel eukaryotic factor for cytosolic Fe-S cluster assembly. *EMBO J.* 2003; 22:4826–4835. [PubMed: 12970194]
24. Netz DJA, Pierik AJ, Stümpfig M, Mühlhoff U, Lill R. The Cfd1-Nbp35 complex acts as a scaffold for iron-sulfur protein assembly in the yeast cytosol. *Nat. Chem. Biol.* 2007; 3:278–286. [PubMed: 17401378]
25. Balk J, Pierik AJ, Netz DJA, Mühlhoff U, Lill R. The hydrogenase-like Nar1p is essential for maturation of cytosolic and nuclear iron-sulphur proteins. *EMBO J.* 2004; 23:2105–2115. [PubMed: 15103330]
26. Balk J, Netz DJA, Tepper K, Pierik AJ, Lill R. The essential WD40 protein Cia1 is involved in a late step of cytosolic and nuclear iron-sulfur protein assembly. *Mol. Cell. Biol.* 2005; 25:10833–10841. [PubMed: 16314508]
27. Kispal G, Csere P, Prohl C, Lill R. The mitochondrial proteins Atm1p and Nfs1p are required for biogenesis of cytosolic Fe/S proteins. *EMBO J.* 1999; 18:3981–3989. [PubMed: 10406803]

28. Klinge S, Hirst J, Maman JD, Krude T, Pellegrini L. An iron-sulfur domain of the eukaryotic primase is essential for RNA primer synthesis. *Nat. Struct. Mol. Biol.* 2007; 14:875–877. [PubMed: 17704817]
29. Burgers PM, Gerik KJ. Structure and processivity of two forms of *Saccharomyces cerevisiae* DNA polymerase δ . *J. Biol. Chem.* 1998; 273:19756–19762. [PubMed: 9677406]
30. Orme-Johnson, WH.; Orme-Johnson, AR. Iron-sulfur proteins. Spiro, TG., editor. Wiley; New York: 1982. p. 67-95.
31. Kent TA, et al. Mössbauer studies of beef heart aconitase: evidence for facile interconversions of iron-sulfur clusters. *Proc. Natl. Acad. Sci. U.S.A.* 1982; 79:1096–1100. [PubMed: 6280166]
32. Tsurimoto T, Stillman B. Multiple replication factors augment DNA synthesis by the two eukaryotic DNA polymerases, α and δ . *EMBO J.* 1989; 8:3883–3889. [PubMed: 2573521]
33. Johansson E, Garg P, Burgers PM. The Pol32 subunit of DNA polymerase delta contains separable domains for processive replication and proliferating cell nuclear antigen (PCNA) binding. *J. Biol. Chem.* 2004; 279:1907–1915. [PubMed: 14594808]
34. Montecucco A, et al. DNA ligase I is recruited to sites of DNA replication by an interaction with proliferating cell nuclear antigen: identification of a common targeting mechanism for the assembly of replication factories. *EMBO J.* 1998; 17:3786–3795. [PubMed: 9649448]
35. Hara K, et al. Crystal structure of human REV7 in complex with a human REV3 fragment and structural implication of the interaction between DNA polymerase ζ and REV1. *J. Biol. Chem.* 2010; 285:12299–12307. [PubMed: 20164194]
36. Dauter Z, Wilson KS, Sieker LC, Moulis JM, Meyer J. Zinc- and iron-rubredoxins from *Clostridium pasteurianum* at atomic resolution: a high-precision model of a ZnS4 coordination unit in a protein. *Proc Natl Acad Sci U S A.* 1996; 93:8836–8840. [PubMed: 8799113]
37. Ramelot TA, et al. Solution NMR structure of the iron-sulfur cluster assembly protein U (IscU) with zinc bound at the active site. *J. Mol. Biol.* 2004; 344:567–583. [PubMed: 15522305]
38. Urzica E, Pierik AJ, Mühlenhoff U, Lill R. Crucial role of conserved cysteine residues in the assembly of two iron-sulfur clusters on the CIA protein Nar1. *Biochemistry.* 2009; 48:4946–4958. [PubMed: 19385603]
39. Nar H, et al. Characterization and crystal structure of zinc azurin, a by-product of heterologous expression in *Escherichia coli* of *Pseudomonas aeruginosa* copper azurin. *Eur. J. Biochem.* 1992; 205:1123–1129. [PubMed: 1576995]
40. Abbouni B, Oehlmann W, Stolle P, Pierik AJ, Auling G. Electron paramagnetic resonance (EPR) spectroscopy of the stable-free radical in the native metallo-cofactor of the manganese-ribonucleotide reductase (Mn-RNR) of *Corynebacterium glutamicum*. *Free Radic. Res.* 2009; 43:943–950. [PubMed: 19707921]
41. Boal AK, Cotruvo JA Jr, Stubbe J, Rosenzweig AC. Structural basis for activation of class Ib ribonucleotide reductase. *Science.* 2010; 329:1526–1530. [PubMed: 20688982]
42. Burgers PMJ. *Saccharomyces cerevisiae* replication factor C. II. Formation and activity of complexes with the proliferating cell nuclear antigen and with DNA polymerases δ and ϵ . *J. Biol. Chem.* 1991; 266:22698–22706. [PubMed: 1682322]
43. Garg P, Stith CM, Majka J, Burgers PMJ. Proliferating cell nuclear antigen promotes translesion synthesis by DNA polymerase ζ . *J. Biol. Chem.* 2005; 280:23446–23450. [PubMed: 15879599]
44. Wong SW, et al. DNA polymerases α and δ are immunologically and structurally distinct. *J. Biol. Chem.* 1989; 264:5924–5928. [PubMed: 2466832]
45. Veatch JR, McMurray MA, Nelson ZW, Gottschling DE. Mitochondrial dysfunction leads to nuclear genome instability via an iron-sulfur cluster defect. *Cell.* 2009; 137:1247–1258. [PubMed: 19563757]
46. Fortune JM, Stith CM, Kissling GE, Burgers PM, Kunkel TA. RPA and PCNA suppress formation of large deletion errors by yeast DNA polymerase δ . *Nucleic Acids Res.* 2006; 34:4335–4341. [PubMed: 16936322]
47. Ayyagari R, Impellizzeri KJ, Yoder BL, Gary SL, Burgers PM. A mutational analysis of the yeast proliferating cell nuclear antigen indicates distinct roles in DNA replication and DNA repair. *Mol. Cell. Biol.* 1995; 15:4420–4429. [PubMed: 7623835]

48. Gomes XV, Gary SL, Burgers PM. Overproduction in *Escherichia coli* and characterization of yeast replication factor C lacking the ligase homology domain. *J. Biol. Chem.* 2000; 275:14541–14549. [PubMed: 10799539]
49. Henricksen LA, Umbricht CB, Wold MS. Recombinant replication protein A: expression, complex formation, and functional characterization. *J. Biol. Chem.* 1994; 269:11121–11132. [PubMed: 8157639]

Author Manuscript

Author Manuscript

Author Manuscript

Author Manuscript

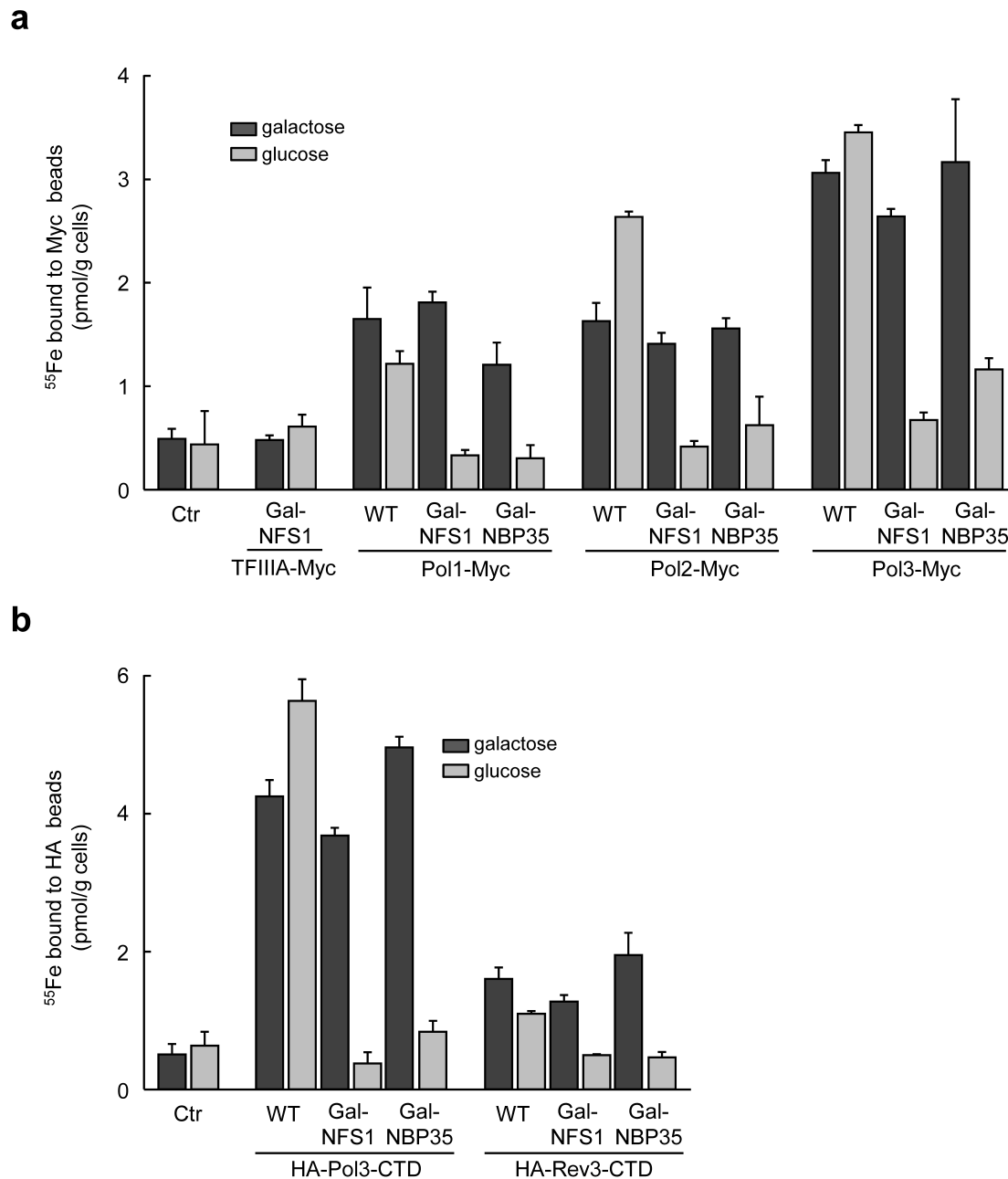


Figure 1. Yeast replicative DNA polymerases (Pol1, Pol2 and Pol3) and Rev3 contain Fe-S clusters *in vivo*

a, Wild-type (WT), Gal-NFS1 or Gal-NBP35 cells harboring genomically Myc-tagged Pol1, Pol2, Pol3, were grown in galactose- (gal) or glucose-containing (glc) medium to induce or repress, respectively, production of Nfs1 or Nbp35. After ⁵⁵Fe radiolabelling of cells, polymerases were immunoprecipitated from cell extracts, and bound ⁵⁵Fe was quantified by scintillation counting. TFIIIA-Myc expressed in Gal-NFS1 and WT cells without tagged polymerases (Ctr) served as controls. **b**, ⁵⁵Fe incorporation into plasmid-encoded HA-Pol3-

CTD and HA-Rev3-CTD as in **a**. Western blots for the cell extracts are presented in **Supplementary Figs. 2 and 6** for **a** and **b**, respectively. Error bars, s.d. (n = 3).

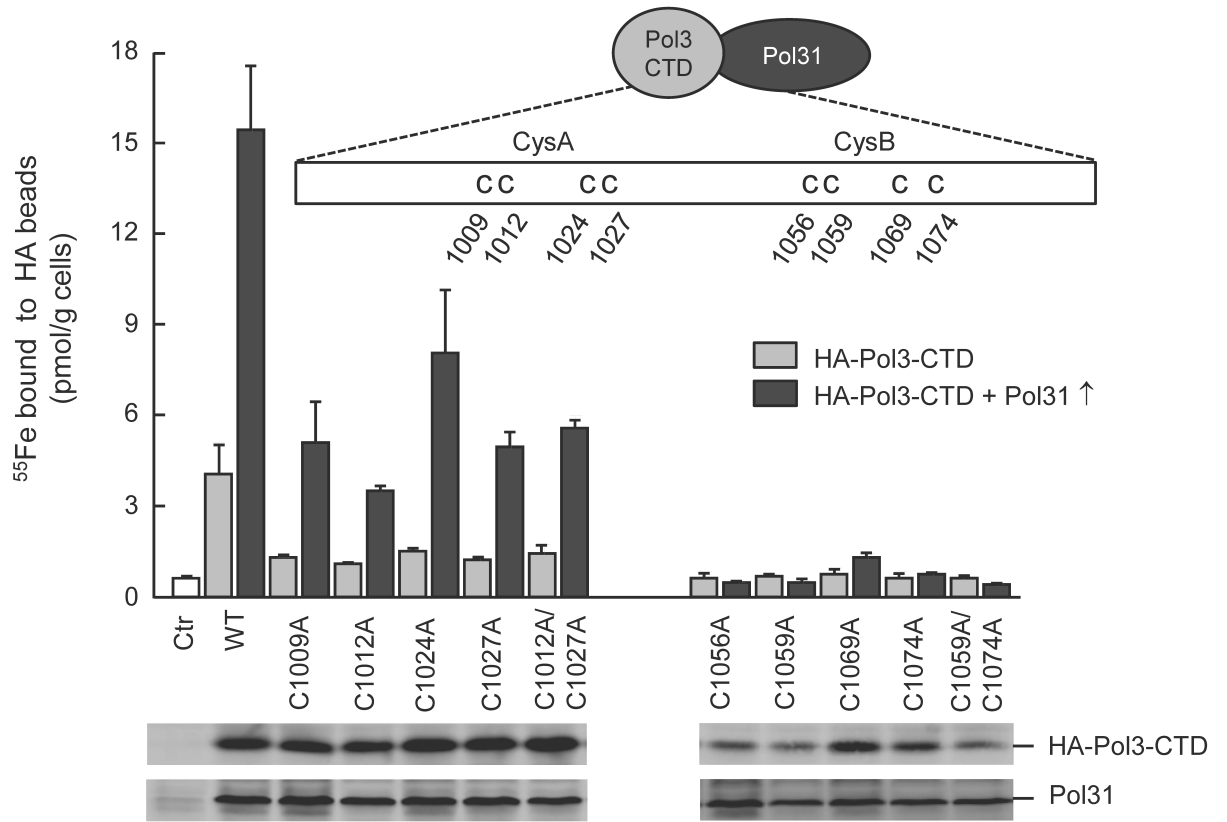
Author Manuscript

Author Manuscript

Author Manuscript

Author Manuscript

a



b

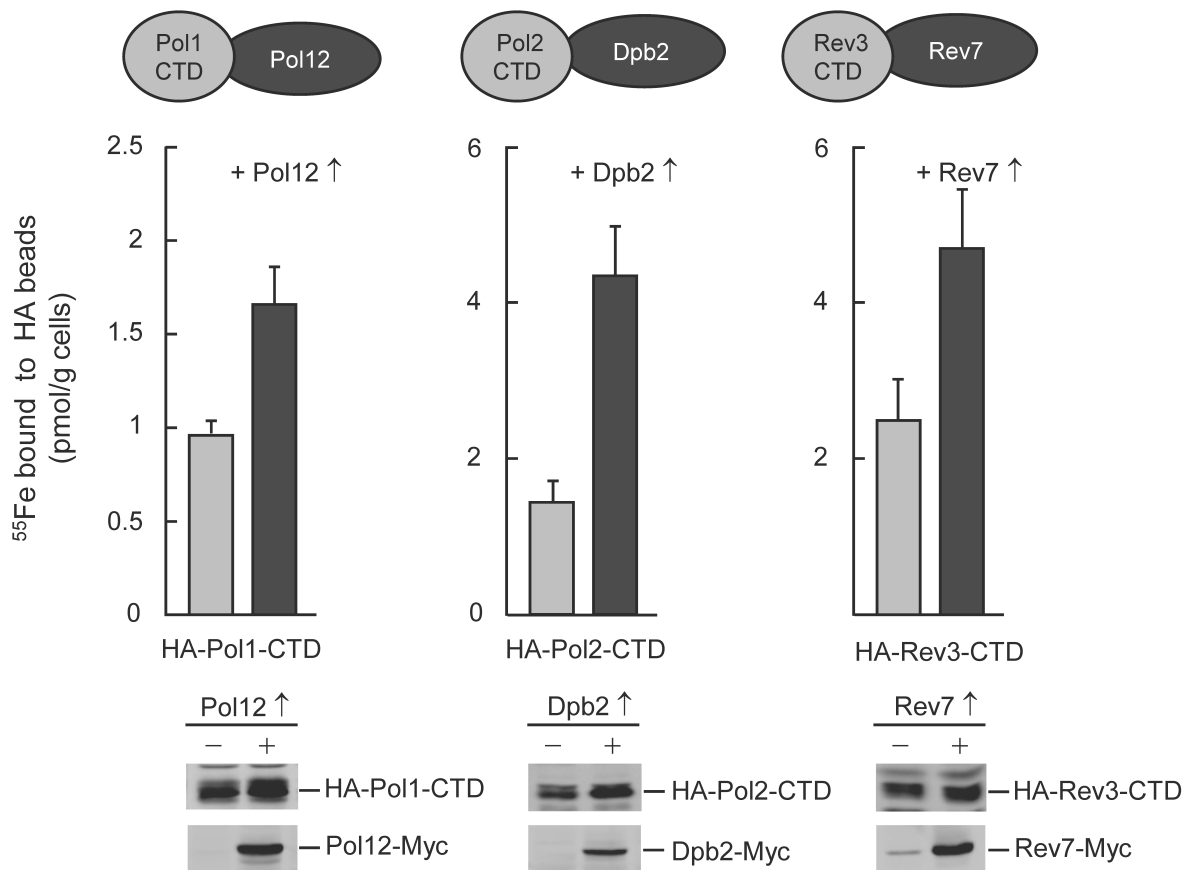


Figure 2. The Fe-S cluster coordinated by the CysB motif of DNA polymerase CTDs is stabilized by binding of the respective accessory subunits

a, ⁵⁵Fe incorporation into plasmid-encoded HA-Pol3-CTD and cysteine to alanine substitutions thereof (cartoon), with (Pol31↑) or without Pol31 over-expression in wild-type yeast cells. Western blots are for cell extracts with Pol31 over-expression. **b**, ⁵⁵Fe incorporation into indicated plasmid-encoded polymerase CTDs, with (↑) or without over-expression of the accessory subunits (cartoon) in wild-type yeast cells. Western blots are shown for indicated cell extracts. Full-length blots are presented in Supplementary Fig. 8. Error bars, s.d. (n = 3).

a

Ctr
Pol1-CTD
Pol2-CTD
Pol3-CTD
Rev3-CTD



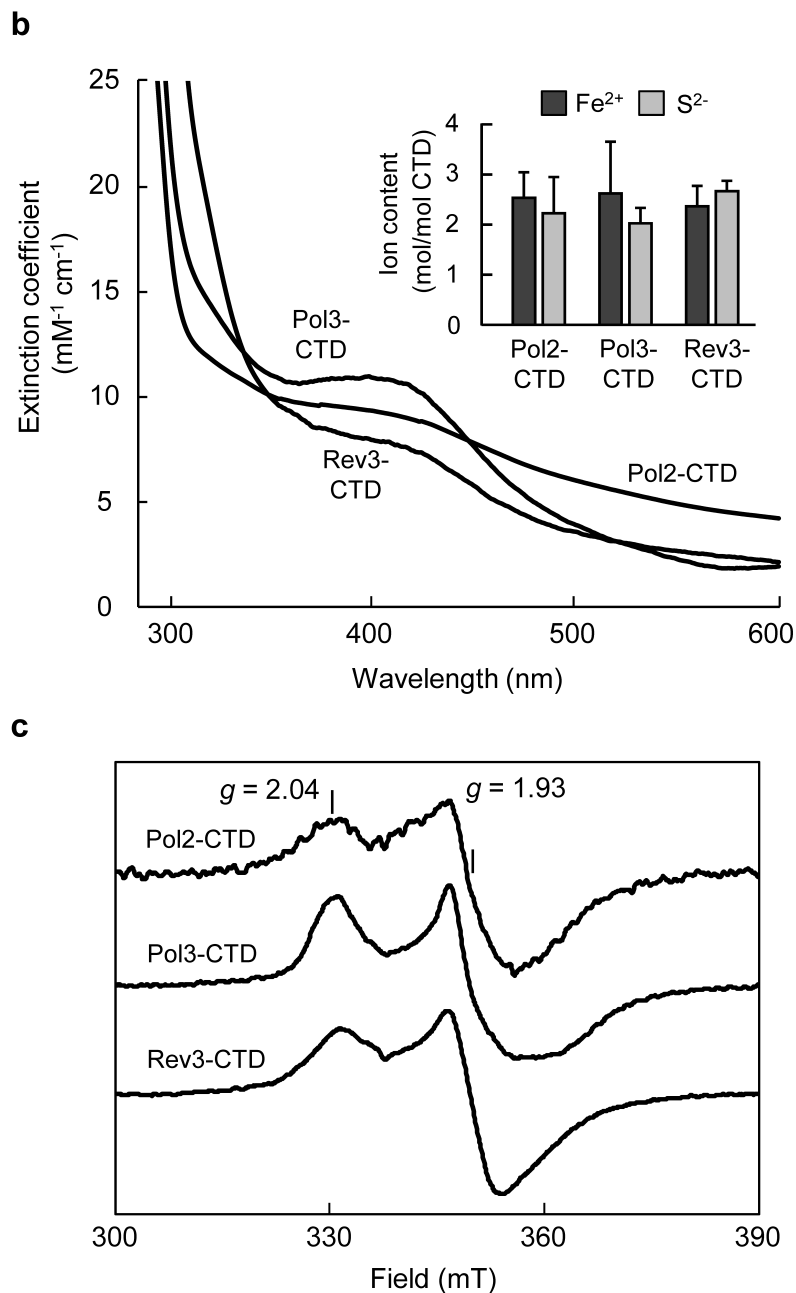


Figure 3. Recombinant purified CTDs of Pol1, Pol2, Pol3 and Rev3 harbour a [4Fe-4S] cluster
a, Solubilized inclusion bodies of indicated CTDs obtained after expression in *E. coli*. **b**, **c**, UV-Vis (**b**) and X-band EPR spectra (**c**) of purified soluble Pol2-, Pol3- and Rev3-CTDs in absence of chaotropic agents. The inset in (**b**) shows non-heme iron and acid-labile sulfide contents. Error bars, s.d. ($n = 3$). Samples in (**c**) were reduced with 2 mM sodium dithionite (2 min), EPR conditions: 9.458 GHz, 10 K and 2 mW microwave power.

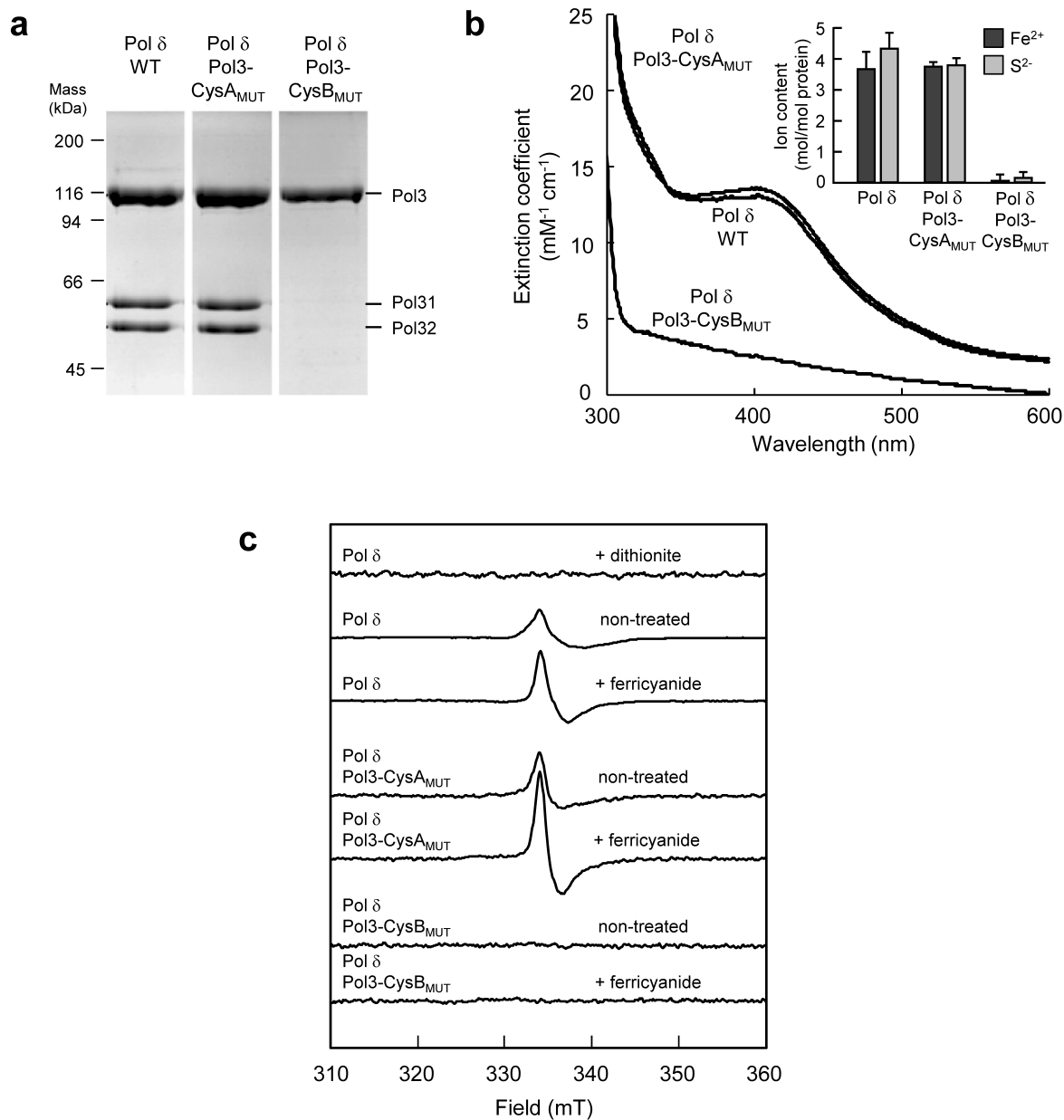
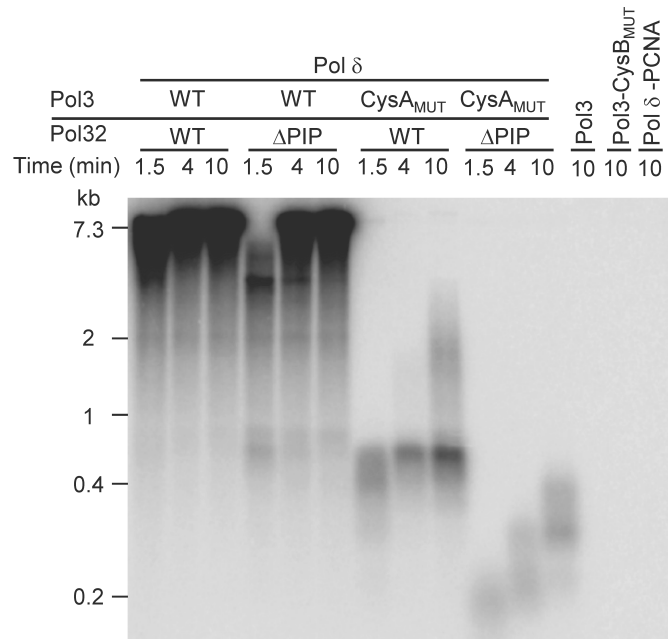


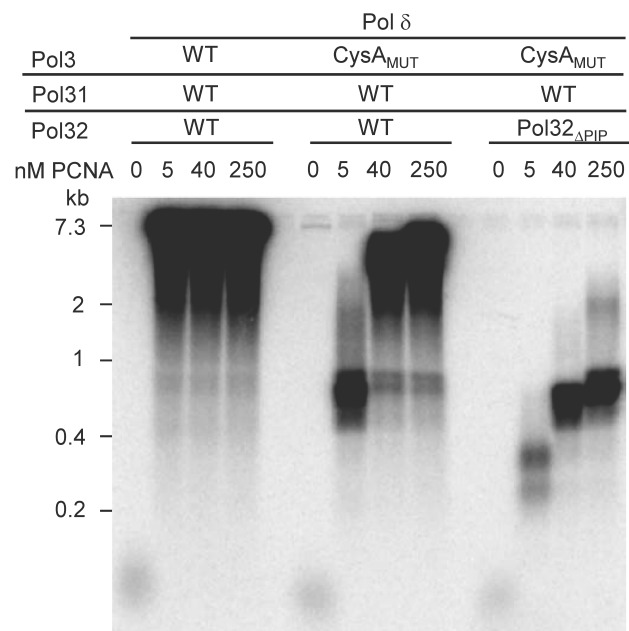
Figure 4. Functional integrity of purified Pol δ complex depends on binding of an Fe-S cluster to Pol3

Pol δ complex purified from yeast co-expressing wild-type (WT), CysA_{MUT} (C1012S/C1027S) or CysB_{MUT} (C1059S/C1074S) Pol3 with Pol31 and Pol32 was analyzed by (a) Coomassie-stained SDS-PAGE, (b) UV-Vis spectroscopy and chemical analysis (inset) or (c) EPR spectroscopy. EPR conditions and treatments with ferricyanide (2 mM) or dithionite are as in Fig. 3c. The full-length gel for a is presented in Supplementary Fig. 11c. Error bars, s.d. (n = 3).

a



b



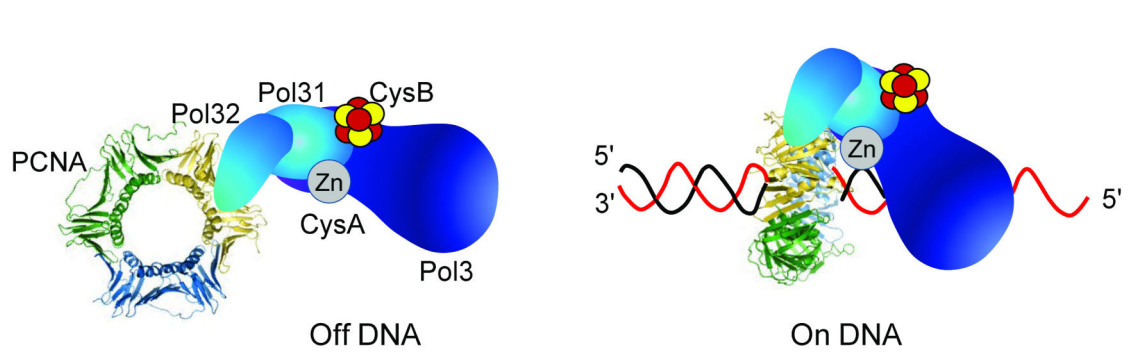


Figure 5. The CysA motif of Pol δ is critical for processive DNA replication with PCNA

a, Alkaline agarose gel electrophoresis of DNA replication products of assay with purified proteins as indicated. A phosphorimaging scan is shown. PIP refers to truncated Pol32 (Supplementary Fig. 11). All complexes contain wild-type Pol31. The right-most lane is a control with WT Pol δ but without PCNA. Size markers are indicated on the left. **b**, Assay as in **a** was carried out for 10 min, and with the indicated PCNA concentrations. **c**, Model for the roles of the PIP and CysA motifs for PCNA interaction with Pol δ in solution (Off DNA), and in assembly with substrate (On DNA).

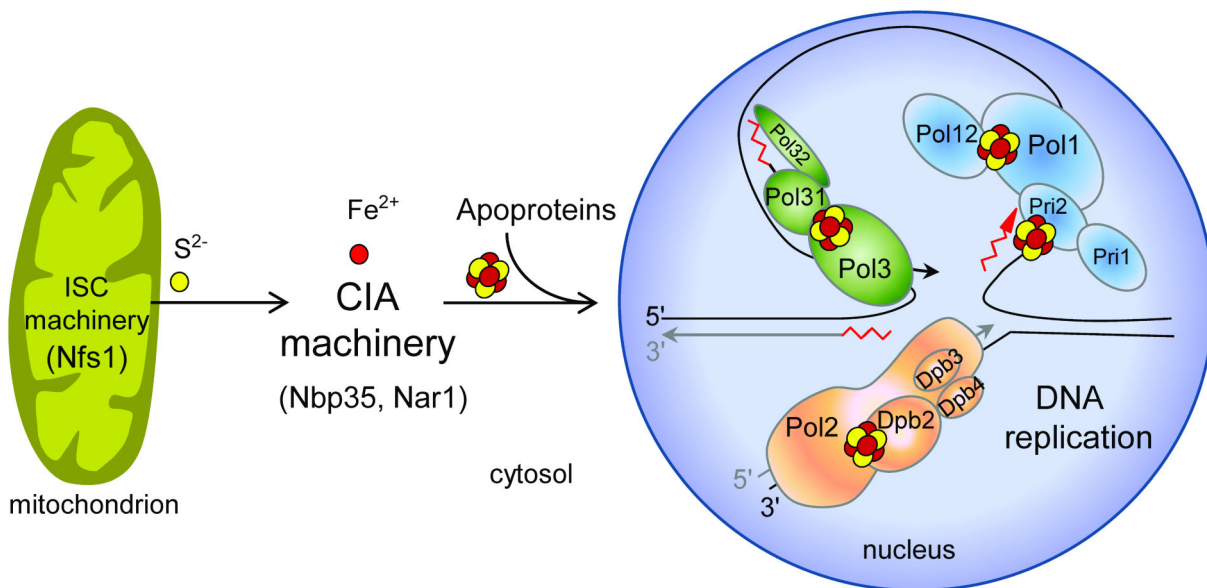


Figure 6. Role of mitochondria and Fe-S cluster biogenesis in nuclear DNA replication
 Assembly of Fe-S clusters on nuclear replicative DNA polymerases requires Fe-S protein biogenesis machineries located in the mitochondria (Iron-Sulfur Cluster assembly, ISC machinery) and cytosol (Cytosolic Iron-sulfur protein Assembly, CIA machinery) providing an explanation for the essential function of mitochondria for cell viability.